



# Monomeric glutaraldehyde fixation and amino acid detoxification of decellularized bovine pericardium for production of biocompatible tissue with tissue-guided regenerative potential

Angélique Lewies<sup>a,\*</sup>, Lezelle Botes<sup>b</sup>, Johannes Jacobus van den Heever<sup>a</sup>, Pascal Maria Dohmen<sup>a,c</sup>, Francis Edwin Smit<sup>a</sup>

<sup>a</sup> Department of Cardiothoracic Surgery, Faculty of Health Sciences, University of the Free State, Bloemfontein, South Africa

<sup>b</sup> Department of Health Sciences, Central University of Technology, Free State, Bloemfontein, South Africa

<sup>c</sup> Department of Cardiac Surgery, Heart Centre Rostock, University of Rostock, Germany

## ARTICLE INFO

### Keywords:

Decellularization  
Bovine pericardium  
Glutaraldehyde fixation  
Amino acids  
Detoxification  
Host cell infiltration  
Calcification  
Bioprosthetic valves

## ABSTRACT

The effect of monomeric glutaraldehyde fixation and amino acid detoxification on biocompatibility and tissue-guided regenerative potential of decellularized bovine pericardium was evaluated. The degree of cross-linking, porosity, enzymatic degradation, alpha-galactosyl content, the efficacy of detoxification, and cytotoxicity towards human epithelial cells were assessed. Tissue was subcutaneously implanted for eight weeks in male juvenile Sprague-Dawley rats, and mechanical properties, host cell infiltration, and calcification were evaluated. Three groups were compared i) decellularized tissue, ii) decellularized, monomeric glutaraldehyde fixed and amino acid detoxified tissue, and iii) commercial glutaraldehyde fixed non-decellularized tissue (Glycar®) (n = 6 rats per group). The fixation process gave a high degree of cross-linking (>85%), and was resistant to enzymatic degradation, with no significant effect on porosity. The detoxification process was effective, and the tissue was not toxic to mammalian cells *in vitro*. Tissue from both decellularized groups had significantly higher ( $p < 0.05$ ) porosity and host cell infiltration *in vivo*. The process mitigated calcification. A non-significant decrease in the alpha-galactosyl content was observed, which increased when including the alpha-galactosidase enzyme. Mechanical properties were maintained. The fixation and detoxification process adequately removes free aldehyde groups and reduces toxicity, preventing enzymatic degradation and allowing for host cell infiltration while mitigating calcification and retaining the mechanical properties of the tissue. This process can be considered for processing decellularized bovine pericardium with tissue-guided regeneration potential for use in cardiovascular bioprostheses; however, methods of further reducing antigenicity, such as the use of enzymes, should be investigated.

## 1. Introduction

Bioprosthetic heart valves (BHVs) entered the market in the mid-1960s as an alternative to mechanical ones, with both valves being an alternative to homografts or allografts [1]. BHVs are the preferred valve implant for children and young adults, as it does not require

\* Corresponding author. Department of Cardiothoracic Surgery, Faculty of Health Sciences, University of the Free State (UFS), (Internal Box G32), P.O. Box 339, Bloemfontein, 9300, South Africa.

E-mail address: [lewiesa@ufs.ac.za](mailto:lewiesa@ufs.ac.za) (A. Lewies).

<https://doi.org/10.1016/j.heliyon.2023.e19712>

Received 1 November 2022; Received in revised form 23 August 2023; Accepted 30 August 2023

Available online 1 September 2023

2405-8440/© 2023 The Authors. Published by Elsevier Ltd. This is an open access article under the CC BY-NC-ND license (<http://creativecommons.org/licenses/by-nc-nd/4.0/>).

long-term anticoagulant therapy. In contrast, lifelong anticoagulant use is mandatory after inserting a mechanical heart valve [2,3]. Bovine pericardium is frequently used in the construction of BHVs [4]. Currently, bovine pericardium is fixed with glutaraldehyde (GA) to provide greater mechanical stability, improve tissue handling, and reduce antigenicity [5,6], with a standard concentration of 0.625% used for fixation [7]. Clinically, bovine pericardial-derived matrixes are also commonly used as a patch for cardiovascular reconstructions [8]. The formation of aneurysmal dilation might be prevented by GA fixation when bovine and autologous pericardium patches are used in the systemic circulation [9].

However, GA fixation prevents the repopulation of the extracellular matrix with host endothelial or interstitial cells and leads to structural deterioration, calcification, and inevitable valve failure [3,10]. Cellular toxicity is associated with the free aldehyde groups of GA, which contributes to preventing the repopulation of tissue with host cells [11]. Furthermore, calcification has been linked to the devitalization of donor cells following GA fixation [12]. The structural valve deterioration and eventual failure of GA-fixed BHVs linked to calcification are age-dependent. Ten percent of GA-fixed BHVs fail within 10 years in patients older than 65 years, whereas a significant rate of failure is observed within 5 years post-implantation in patients younger than 35 years [13].

Anti-calcification strategies include the detoxification of GA-fixed tissue using amino acid solutions which bind the free aldehyde groups, improving the durability and biocompatibility of tissue [14]. Polyols, such as propylene glycol, which bind to free aldehyde groups to mitigate calcification, has been used to treat commercially available GA-fixed bovine pericardium patches (Glycar® patches) [15]. GA solutions consist of a mixture of monomers and polymers. The use of monomeric GA in cross-linking allows for the benefit of lowering concentrations of the fixative to achieve adequate cross-linking of tissue [16]. Delipidation and/or decellularization strategies have been developed to mitigate the calcification of bovine pericardium [17–19]. Decellularization involves the removal of host cells and nuclear material while keeping the extracellular matrix intact [20]. An advantage of decellularization is that it can also reduce the antigenicity associated with xenograft tissue and promote tissue longevity [21,22].

Tissue-guided regeneration is a modality of tissue engineering adopted in cardiovascular regenerative medicine [23]. The concept was initially introduced in dental and bone bioengineering and referred to when biomimetic scaffolds are implanted and able to stimulate themselves for the regeneration process to take place without biological signals [24]. In contrast to traditional tissue engineering concepts where living tissue is created *in vitro*, tissue-guided regeneration infers that the body is the bioreactor and that adaptive remodeling and healing occur through natural physiological conditioning and the host's cell recruitment and engraftment [23].

This study aimed to develop a fixation and detoxification process for decellularized bovine pericardium that produces biocompatible tissue with tissue-guided regenerative potential for use in cardiovascular bioprotheses. We evaluated the effectiveness of using a low concentration (0.05%) of monomeric GA for the fixation of decellularized bovine pericardium, followed by amino acid detoxification to maintain mechanical stability (strength and stiffness) and prevent calcification. Furthermore, the effectiveness of the fixation and detoxification process in reducing antigenicity, lowering cytotoxicity, and promoting host cell recruitment and infiltration following the subcutaneous implant of the tissue in juvenile rats was evaluated.

## 2. Materials and methods

### 2.1. Study design

The study was divided into an *in vivo* and *in vitro* phase (Fig. 1). Decellularized tissue was fixed using GA or monomeric GA. The degree of cross-linking, resistance to enzymatic degradation, porosity and alpha-galactosyl ( $\alpha$ -gal) content were evaluated. Following fixation, the detoxification efficacy of an amino acid solution was compared to propylene glycol. Finally, the cytotoxicity of the fixed and detoxified tissue towards a human epithelial cell line was assessed. These results determined the optimal process for fixing and detoxifying decellularized bovine pericardium using monomeric GA and an amino acid solution. Tissue processed using this method was subcutaneously implanted into a juvenile rat model to evaluate calcification, host cell infiltration, and mechanical properties (Tensile Strength and Young's Modulus (stiffness)). A decellularized group and a commercial tissue (Glycar®) were included for comparison.

### 2.2. Materials

All reagents used were of analytical grade and were purchased from Sigma-Aldrich, Johannesburg, South Africa (SA), unless otherwise specified. Freshly slaughtered bovine pericardial sacs from young animals were obtained from a local abattoir (Bloemfontein Abattoir, Free State, SA). A human epithelial cell line (HEK cells from American Type Culture Collection (ATCC®CRL-1573™)) was used for cytotoxicity assays. Juvenile male Sprague-Dawley rats were bred by the Vivarium of the Preclinical Drug Development Platform of the North-West University (NWU) in Potchefstroom, SA, and sourced by the Animal Research Centre, University of the Free State, Bloemfontein, SA. Rats were used for the subcutaneous implant of tissue. The interfaculty Animal Ethics Committee (UFS-AED2020/0067) and Environmental and Biosafety Ethics Committee (UFS-ESD2020/0153) of the University of the Free State approved the study.

### 2.3. Processing of tissue

Bovine pericardial sacs were transported on ice to the laboratory and manually stripped free of attached fat and adventitial tissue while being washed in cold (4 °C) Ringers-Lactate solution (Fresenius Kabi/Intramed, Midrand, SA) to get rid of excess blood. The

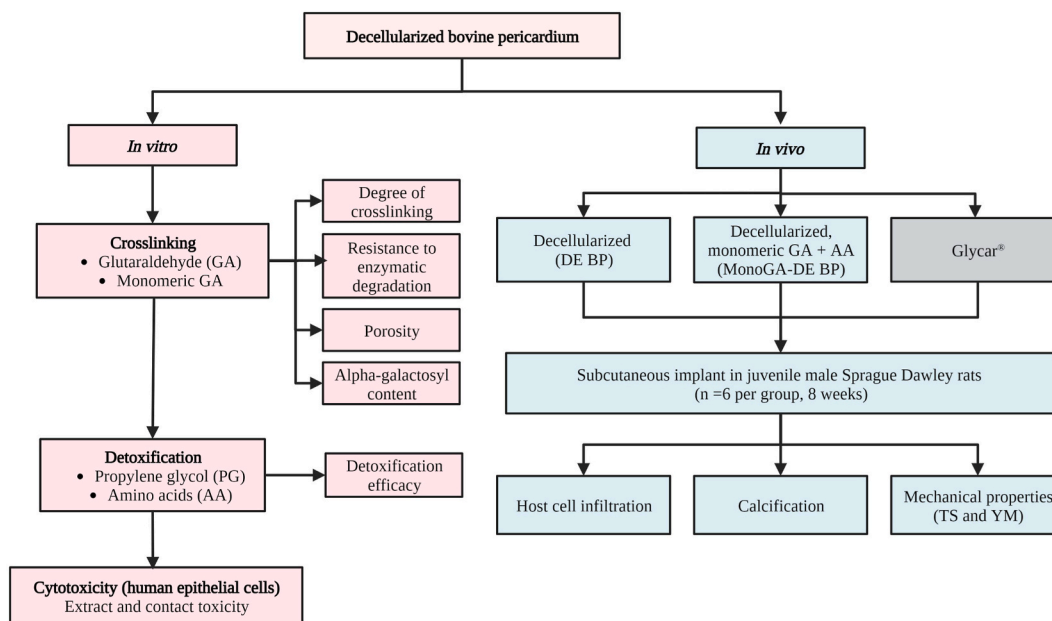


**Fig. 1.** Study design. Where; TS, Tensile strength; YM; Young's modulus.

bovine pericardium was decellularized using a proprietary decellularization protocol [25]. Bovine pericardium patches were submerged in an antibiotic and antimycotic solution (2.5 mg Amphotericin B, 50 mg Piperacillin, 50 mg Vancomycin and 25 mg Amikacin sulphate). The pericardium was then subjected to osmotic shock, repeated changes in a multi-detergent solution (0.5% sodium dodecyl sulphate (SDS), 1% sodium deoxycholate (SDC), 1% Triton-X100) and numerous washings in PBS and half-strength antibiotic and antimycotic solution as well as 40 µg/ml IturinA under constant shaking. Delipidation was done with 70% ethanol.

Monomers and polymers coexist in glutaraldehyde (GA) solutions. The fixation properties of GA are influenced by the ratio of monomers to polymers [26] Commercial GA (technical grade GA) is a mixture of monomeric dialdehyde and impurities attributable to polymerization. Monomeric GA has a UV-visible spectrophotometry absorbance peak at 280 nm, while polymeric materials absorb at 235 nm [27]. Two variations of GA were used in this study, to crosslink (fix) decellularized bovine pericardium, namely.

- (i) 0.625% GA technical grade, which contains both monomeric and polymeric groups (absorbance peaks at 235 nm)
- (ii) 0.05% monomeric GA, which was purified from technical grade GA through glass distillation (no absorbance peak at 235 nm) (Polysciences, Inc. USA).

GA and monomeric GA fixation was done in phosphate buffer ( $\text{KH}_2\text{PO}_4$ , pH 7.4) for 72 h at 4 °C, followed by the addition of hydrogen peroxide ( $\text{H}_2\text{O}_2$ ) in phosphate buffer for 4 h at 4 °C. Following fixation, tissue was detoxified using 100% propylene glycol [28] or an amino acid solution containing 0.1 M glycine [29].

Groups of processed bovine pericardium were classified as follows.

- (i) DE BP: decellularized bovine pericardium
- (ii) GA-DE BP: decellularized bovine pericardium fixed with GA and detoxified with an amino acid solution
- (iii) MonoGA-DE BP: decellularized bovine pericardium fixed with monomeric GA and detoxified with an amino acid solution

For each group, n = 6 samples were prepared and analyzed. DNA was extracted from tissue using a QIAamp® DNA Mini Kit (QIAGEN Johannesburg, SA), and the complete decellularization of tissue was confirmed by measuring the DNA content (ng DNA/mg tissue) using a BioDrop spectrophotometer (Biochrom Ltd., Cambridge, UK). Acellularity was also confirmed with hematoxylin and eosin (H&E) staining. All tissue was confirmed to be culture negative (anaerobic and aerobic bacteria, fungi, and yeast) after processing by a registered pathology laboratory PathCare Veterinary Laboratory (Bloemfontein, SA). The commercially available Glycar® bovine pericardial patch (Glycar Pty Ltd, Irene, South Africa) was used in *in vivo* experiments as a control. This patch is not decellularized, GA tanned (0.625%), formaldehyde (4%) sterilized, detoxified with propylene glycol (100%), and stored in propylene oxide (2%).

## 2.4. In vitro phase

### 2.4.1. Evaluating the degree of cross-linking

The degree of cross-linking is considered to be the ratio of the bound amine groups in the cross-linked (fixed) decellularized tissue to the free amine groups from the unfixed decellularized tissue and was determined using the ninhydrin assay [30]. Pericardial tissue (n = 6 per group) was air-dried and homogenized using a G50 Motor-Driven Tissue Grinder (Coyote Biosciences Inc., USA) in lysis buffer (150 mM NaCl, 1% Triton-X 100, 0.5% SDS, 0.1% SDC, 50 mM Tris-HCl, protease inhibitor). A 2% ninhydrin solution was added to the homogenate, which was then heated at 80 °C for 20 min. The samples were then cooled to room temperature and diluted 1:5 with 50% isopropanol. The number of free amine groups was determined by measuring the optical absorbance of the solution at 570 nm with a microplate reader (BioTEK, Synergy HT with Gen5.1.1 software). The concentration of the free amine groups was determined by a standard curve of glycine concentration vs. absorbance. The degree of cross-linking was calculated using equation (1).

$$\text{Degree of Crosslinking} = \frac{(M_o - M_t)}{M_o} \times 100 \% \quad (1)$$

where;  $M_o$  is the number of free amine groups in the non-cross-linked tissue, and  $M_t$  is the number of amine groups remaining in the cross-linked tissue, both normalized to tissue weight [28]. Decellularized tissue fixed with decreasing concentrations (0.625%, 0.1%, and 0.05%) of monomeric GA without the addition of  $H_2O_2$  was included for comparison.

### 2.4.2. Evaluation of the enzymatic degradation of tissue

A ninhydrin-based collagenase assay was used to determine the enzymatic degradation of tissue [31]. Tissue was air dried, and 10–20 mg of tissue was added to 2 ml of a collagenase solution (0.01 mg/ml Collagenase enzyme (Type 1A) in a buffer containing 50 mM N-tris[hydroxymethyl]methyl-2 aminoethane sulfonic acid (TES) and 25 mM calcium chloride, pH 7.4). The samples were incubated at 37 °C for 24 h. A ninhydrin assay was performed by adding 100  $\mu$ l of the collagenase solution to 400  $\mu$ l of 2% ninhydrin solution and heating it at 80 °C for 20 min. The samples were then cooled to room temperature and diluted 1:5 with 50% isopropanol. The amount of soluble collagen peptides produced by the action of the collagenase enzyme was determined by measuring the absorbance of the solution at 570 nm with a microplate reader (BioTEK, Synergy HT with Gen5.1.1 software). The absorbance of the sample was divided by the weight of the tissue giving an OD/mg value. This OD/mg value represents the amount of collagen peptides degraded by the action of the collagenase enzyme. Glycar® patches were included for comparison.

### 2.4.3. Evaluation of the porosity of tissue

Tissue samples were collected in 3% buffered GA and processed according to the standard scanning electron microscopy (SEM) evaluation protocols described in Ref. [32]. SEM samples were visually assessed using a Shimadzu SSX -550 scanning electron microscope (Kyota, Japan). Porosity was evaluated using ImageJ version 1.52t software (National Institute of Health, Bethesda, Maryland, USA, <https://imagej.nih.gov/ij/>). Glycar® patches were included for comparison.

### 2.4.4. Evaluation of the alpha-galactosyl ( $\alpha$ -gal) content of tissue

The  $\alpha$ -gal content (ng/ml) of processed tissue was evaluated using a Bovine  $\alpha$ -gal ELISA kit (MyBioSource.com, USA). Tissue was air dried, and 15–20 mg of tissue was weighed and homogenized in 0.5 ml of RIPA lysis buffer (10 mM Tris-HCl, 1 mM EDTA, 0.5 mM EGTA, 1% Triton X-100, 0.1% SDC, 0.1% SDS, 140 mM NaCl and 1 mM PMSF) [33]. The ELISA was performed according to the instructions of the manufacturer using undiluted samples. Absorbance was measured at 450 nm with a microplate reader (BioTEK, Synergy HT with Gen5.1.1 software). Following the homogenization of the tissue, the Pierce™ BCA Protein assay Kit (Thermo Fisher Scientific, USA) was used to determine the amount of protein ( $\mu$ g/ml) in each sample according to the manufacturer's instructions for the microplate procedure. Absorbance was measured at 562 nm with a microplate reader (BioTEK, Synergy HT with Gen5.1.1 software). Results were expressed as ng alpha-galactosyl/mg protein. Processed tissue was compared to the fresh native unprocessed bovine pericardium. Tissue treated with 0.5 U/ml  $\alpha$ -galactosidase from green coffee beans in 100  $\mu$ M HEPES buffer for 24 h at 25 °C on an orbital shaker at 200 rpm and Glycar® patches were included for comparison.

### 2.4.5. Evaluating the detoxification efficacy

Fuchsin staining was performed to detect free aldehyde groups in the GA-DE BP and MonoGA-DE BP groups following detoxification (n = 6 per group). GA fixed decellularized tissue was also detoxified with propylene glycol for comparison. Positive controls were included for each group, which was fixed and only rinsed with saline. An acidic solution of rosaniline hydrochloride (fuchsin) was used [34]. Samples were immersed in stain (1% rosaniline hydrochloride, 4% sodium metabisulfite in 0.25 M hydrochloric acid (HCl)), transferred and immersed into a wash solution (8 g of  $Na_2SO_3$  and 0.4 M HCl), followed by two successive washes in acidic ethanol. The tissue was placed in phosphate-buffered saline pH 7.4 and photographed using a digital camera. The samples were then dried and homogenized in DMSO using a G50 Motor-Driven Tissue Grinder (Coyote Biosciences Inc., USA). The absorbance of the resulting solution was measured at 570 nm in a microplate reader (BioTEK, Synergy HT with Gen5.1.1 software) to quantify the staining intensity (level of free aldehydes).

#### 2.4.6. Contact and extract toxicity of processed tissue

**2.4.6.1. Cell culturing conditions.** Cells were cultured, and experiments were performed under standard conditions in Dulbecco's modified essential medium (DMEM, Lonza, Basel, Switzerland) containing 10% fetal bovine serum (FBS, HyClone™, GE Healthcare, South Logan, USA), 1% penicillin/streptomycin (Lonza, Basel, Switzerland), 2 mM L-Glutamine (Lonza, Basel, Switzerland) and 1% non-essential amino acids (Lonza, Basel, Switzerland). Cells were cultured, and experiments were performed at  $37 \pm 2$  °C,  $95 \pm 2$  % humidified atmosphere of 5% CO<sub>2</sub>. Cells were passaged with 1% Trypsin/EDTA (Lonza, Basel, Switzerland).

**2.4.6.2. Contact toxicity.** The cytotoxicity of the GA-DE BP and MonoGA-DE BP groups was determined based on their direct contact or due to leach-ables per ISO 10993–5:2009 (n = 6 per group). Pieces of tissue (5 × 10 mm) were rinsed with sterile 1 × phosphate-buffered saline (PBS) and attached to the bottom of a 12-well plate (Nest Biotechnology Co., Ltd, China) using cell culture grade collagen from rat tail tendon (Roche Diagnostics GmbH, Mannheim, Germany). HEK cells were seeded at 200 000 cells per well in complete cell culture media. Plates were incubated for 48 h. Cell culture plates were microscopically examined for cellular response around the tissue samples. The pieces of tissue were collected and placed in 4% buffered formalin and H&E stained. All images were captured using a Motic® AE31 Inverted Microscope fitted with a MotiCam X<sup>3</sup> and MotiConnect imaging software (Motic China Group, Ltd, China).

**2.4.6.3. Extract toxicity.** Extract toxicity of the GA-DE BP and MonoGA-DE BP groups was performed per ISO 10993–5:2009 (n = 6 per group). Unprocessed native tissue was used as a control. Tissue was rinsed with sterile 1 × PBS and minced, and 0.1 g of tissue/1 ml of complete cell culture media was incubated for 24 h at 37 °C with agitation (200 rpm). Samples were centrifuged at 10 000 rpm for 10 min, and the supernatants were collected. HEK cells were seeded at 15 000 cells per well in 96-well plates (Nest Biotechnology Co., Ltd, China) and allowed to reach sub-confluence. Cell culture media was removed, replaced with the tissue extracts supernatants, and incubated for 48 h. The 3-(4,5-dimethylthiazol-2-yl)-2,5-diphenyl tetrazolium bromide (MTT) assay was performed as described in Ref. [35]. Absorbance was measured at 570 nm and background at 650 nm, with DMSO measured as a blank. Blank and background measurements were subtracted, and cell viability was expressed as a percentage relative to native (unprocessed) tissue, which was set as 100% viable. A positive control consisting of extracts made from decellularized tissue fixed with 0.625% GA, not detoxified, and not rinsed was included.

#### 2.5. Implantation and evaluation of tissue in a subcutaneous rat model (In vivo phase)

##### 2.5.1. Animal housing

All animal experiments and surgical procedures comply with Animals in Research: Reporting In Vivo Experiments (ARRIVE) guidelines [36] and were performed in compliance with the South African National Standard for the care and use of animals for scientific purposes (SANS 10386:2008). Juvenile male Sprague-Dawley rats (n = 18) with a mean weight of  $151.17 \pm 28.93$  g (5–6 weeks of age) [37] were housed in a temperature and humidity-controlled ( $22 \pm 2$  °C and  $55 \pm 15$  % relative humidity) animal facility (Animal Research Centre, University of the Free State, Bloemfontein) with 12h light/dark cycles. Only males were used in this study to avoid gender-based related differences. Two rats were kept per polysulfone cage (56x35 × 20 cm (WxDXH)) with pinewood shaving bedding. Rats had *ad libitum* access to food and demineralized water.

##### 2.5.2. Subcutaneous implant and explant of tissue

Three groups of tissue were implanted, i) DE BP, ii) MonoGA-DE BP, and iii) commercial GA fixed non-decellularized tissue (Glycar®) (n = 6 rats per group, n = 18 total number of rats). Rats were randomly assigned to a tissue group, and two implants (1 × 4 cm) of the respective tissue were subcutaneously implanted on their backs (n = 12 specimens per group, n = 6 used for the evaluation of host cell infiltration and calcification and n = 6 used to evaluate mechanical properties of the tissue). Anesthesia was induced by 5% isoflurane and maintained at 2% isoflurane. Rats were shaved and cleaned with F10 Skin Prep Solution (Health and Hygiene (Pty) Ltd., South Africa), and buprenorphine (0.05 mg/kg) was injected subcutaneously. A midline incision of ±4 cm was made through the skin on the back. Two pre-cut pericardial samples from each group were rinsed for 15 min in sterile 0.9% saline (Adcock Ingram, Johannesburg, South Africa) before implantation. The tissue was inserted subcutaneously into separate pockets made on the back (one on each side) of the animal and secured with four 6/0 Prolene sutures. The incision was closed with a continuous 5/0 PDS absorbable suture. On completion of the eight weeks implantation period, all the animals were euthanized through the intraperitoneal injection of sodium pentobarbital (200 mg/kg) under isoflurane sedation. Tissue implants were collected for measurement of host cell infiltration, calcification, and strength and stiffness analysis.

##### 2.5.3. Evaluation of host cell infiltration

Tissue samples were collected in 4% buffered Formalin, embedded in paraffin wax, sectioned, and stained according to standard H&E protocols [38]. The histology of the explants was compared to that of similarly processed pre-implanted tissue. Cell counts were performed on H&E images with ImageJ version 1.52t software (National Institute of Health, Bethesda, Maryland, USA, <https://imagej.nih.gov/ij/>).

### 2.5.4. Evaluation of calcification

Qualitative calcium was evaluated with von Kossa staining. Tissue samples were collected in 4% buffered formalin, embedded in paraffin wax, sectioned, and stained according to standard von Kossa protocols [39]. The calcification of the explants was compared to similarly processed pre-implanted tissue. Quantitative calcium analysis was performed using inductively coupled plasma mass spectrometry (ICP-MS), as described in Ref. [40].

### 2.5.5. Evaluation of the mechanical properties

The mechanical properties (Tensile strength (TS) and Young's Modulus (YM)) of the bovine pericardium tissue were uniaxially assessed at room temperature by an automated and computerized TS testing apparatus (Lloyds LS100 Plus, IMP, SA). Pre-implantation tissue and tissue at explant were cut (5 × 40 mm). The average thickness was calculated from thickness measured at three different locations along the center of the strip using a MiniTest 137-735-F5HD thickness gauge (ElectroPhysik, Germany). Both ends of the tissue strips were fixed between two grips (Mark-10 Corporation, USA) and gradually stretched at 0.1 mm/s, applying constant tension on the two ends. Force was calculated using a 500 N load cell. Native bovine pericardium samples were also analyzed. The TS (MPa) and YM (MPa) or modulus of elasticity were calculated from the stress-strain curve using Nexygen Plus 3 software (Lloyd Instruments, IMP, Johannesburg SA).

## 2.6. Statistical analysis

Statistical analyses were performed using GraphPad Prism version 9.3.1 (GraphPad Software, La Jolla, CA, USA). Due to the explorative nature of the study, the resource equation approach, which sets the acceptable range of the error degrees of freedom (DF) in an analysis of variance (ANOVA), was used to calculate the number of animals required (i.e. for sample size calculations) [41]. Based on these calculations,  $n = 6$  animals per group were included (to keep the DF within the range of 10–20). Results were expressed as medians with corresponding ranges (first and third quartiles). Where applicable, continuous values were subjected to a Kruskal-Wallis (KW) multiple comparison analysis with Dunn's posthoc test to make individual comparisons between groups. For two group comparisons, the Wilcoxon signed-rank test was used to measure differences between dependent groups, and the Mann-Whitney  $U$  Test was used to measure differences between independent groups. Cytotoxicity results were expressed as a percentage relative to the control using mean  $\pm$  standard deviation and evaluated using a one-way analysis of variance (ANOVA) with Dunnett's multiple comparisons posthoc test. Significance was set as  $p < 0.05$ .

## 3. Results

### 3.1. Acellularity of tissue

All cells were removed from native tissue following decellularization, as shown with H&E (Fig. 2 A and B). The DNA content of native tissue before decellularization was 228.6 ng DNA/mg tissue (range 162.6–323.7 ng DNA/mg tissue), and for decellularized tissue, it was significantly lower ( $p = 0.0001$ ) at 24.48 ng DNA/mg tissue (range 20.72–26.33 ng DNA/mg tissue) (Fig. 2C).

### 3.2. Degree of cross-linking

The degree of cross-linking decreased as the monomeric GA concentration decreased (Fig. 3); however, this decrease was not significant. Adding  $H_2O_2$  to the fixation solution significantly increased the cross-linking achieved using 0.05% monomeric GA ( $p = 0.004$ ). No significant difference ( $p = 0.977$ ) was found between the degree of cross-linking achieved when using 0.625% GA (83.81% (range 82.34–86.4%)) and using 0.05% monomeric GA plus  $H_2O_2$  (88.93% (range 86.09–98.18%)). Henceforward,  $H_2O_2$  was included in the fixation process when using 0.05% monomeric GA, and all instances where monomeric GA is mentioned include the use of  $H_2O_2$ .

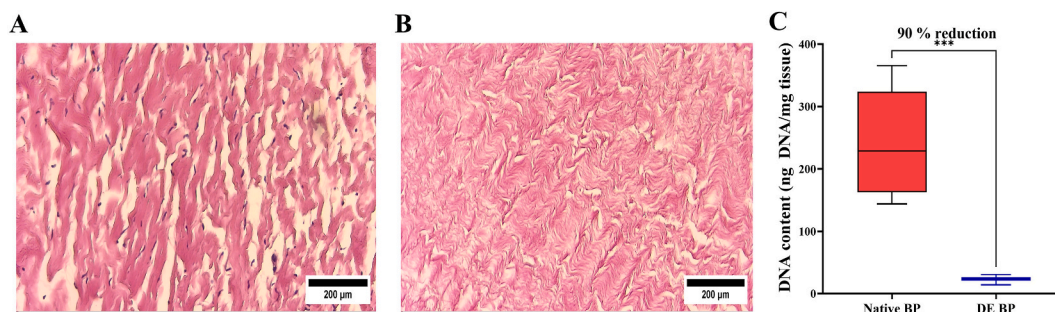


**Fig. 2.** Confirmation of acellularity of decellularized bovine pericardium. Representative hematoxylin and eosin stains (light microscope images) of (A) native tissue and (B) decellularized tissue (200 × magnification, scale bars 200  $\mu$ m) and (C) DNA content expressed as ng DNA/mg tissue ( $n = 6$ ). Where: Native BP, unprocessed bovine pericardium; DE BP, decellularized bovine pericardium \*\*\* $p < 0.001$ .

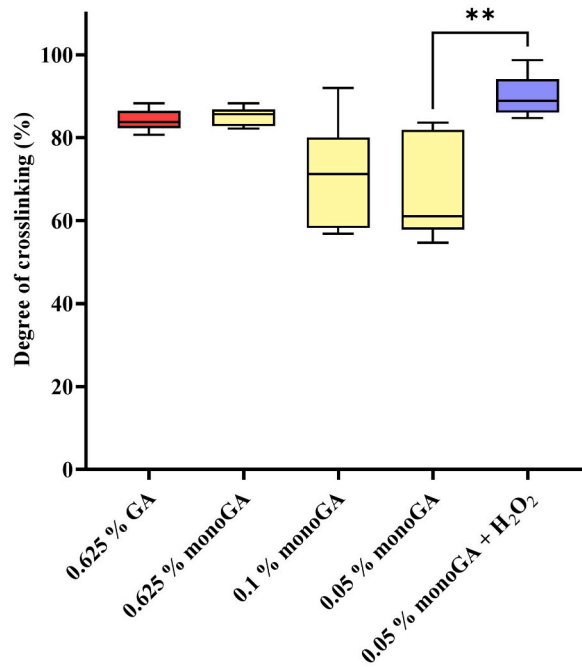


**Fig. 3.** Degree of cross-linking determined with the ninhydrin analysis (n = 6). Where: GA, glutaraldehyde; monoGA, monomeric glutaraldehyde, H<sub>2</sub>O<sub>2</sub>, hydrogen peroxide. \*\*p < 0.01.

### 3.3. Effect of cross-linking on the enzymatic degradation of tissue

Enzymatic degradation was evaluated through a ninhydrin-based collagenase assay. The DE BP group had the highest susceptibility to enzymatic degradation (0.0227 OD/mg (range 0.0115–0.0299) (Fig. 4). The number of collagen peptides degraded by the action of

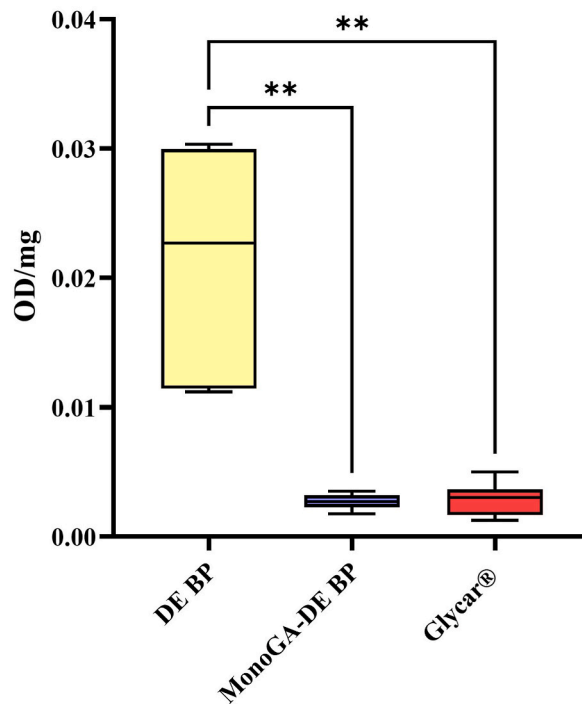


**Fig. 4.** Enzymatic degradation of tissue determined through a ninhydrin-based collagenase assay (n = 6). Where: DE BP, decellularized bovine pericardium; MonoGA-DE BP, decellularized bovine pericardium fixed with monomeric glutaraldehyde. \*\*p < 0.01.

the collagenase enzyme was significantly higher for the DE BP group compared to the MonoGA-DE BP ( $p = 0.0049$ ) and the Glycar® ( $p = 0.0098$ ) groups (Fig. 4).

### 3.4. Effect of cross-linking on porosity

Porosity was calculated from the SEM images (Fig. 5. A). The porosity of the DE BP group was found to be the highest (34.15% (range 26.94–44.79%)) (Fig. 5. B). The porosity of GA-DE BP and Glycar® groups was significantly lower than that of the DE BP group ( $p = 0.0079$  and  $p = 0.0006$ , respectively) (Fig. 5. B). The porosity of the MonoGA-DE BP group did not differ significantly from that of the DE group ( $p > 0.9999$ ); however, the MonoGA-DE BP group's porosity was significantly higher than that of the Glycar® group ( $p = 0.0039$ ) (Fig. 5. B).

### 3.5. Alpha-galactosyl content of tissue

Compared to fresh, unprocessed native bovine pericardium the DE BP, MonoGA-DE BP and Glycar® groups had a lower  $\alpha$ -gal content. However, the decrease was not found to be significant ( $p > 0.05$ ) (Fig. 6). The addition of 0.5 U/ml  $\alpha$ -galactosidase did lead to a significant decrease in the  $\alpha$ -gal content of the DE BP group ( $p = 0.0018$ ) and the MonoGA-DE BP group ( $p = 0.0029$ ) (Fig. 6).

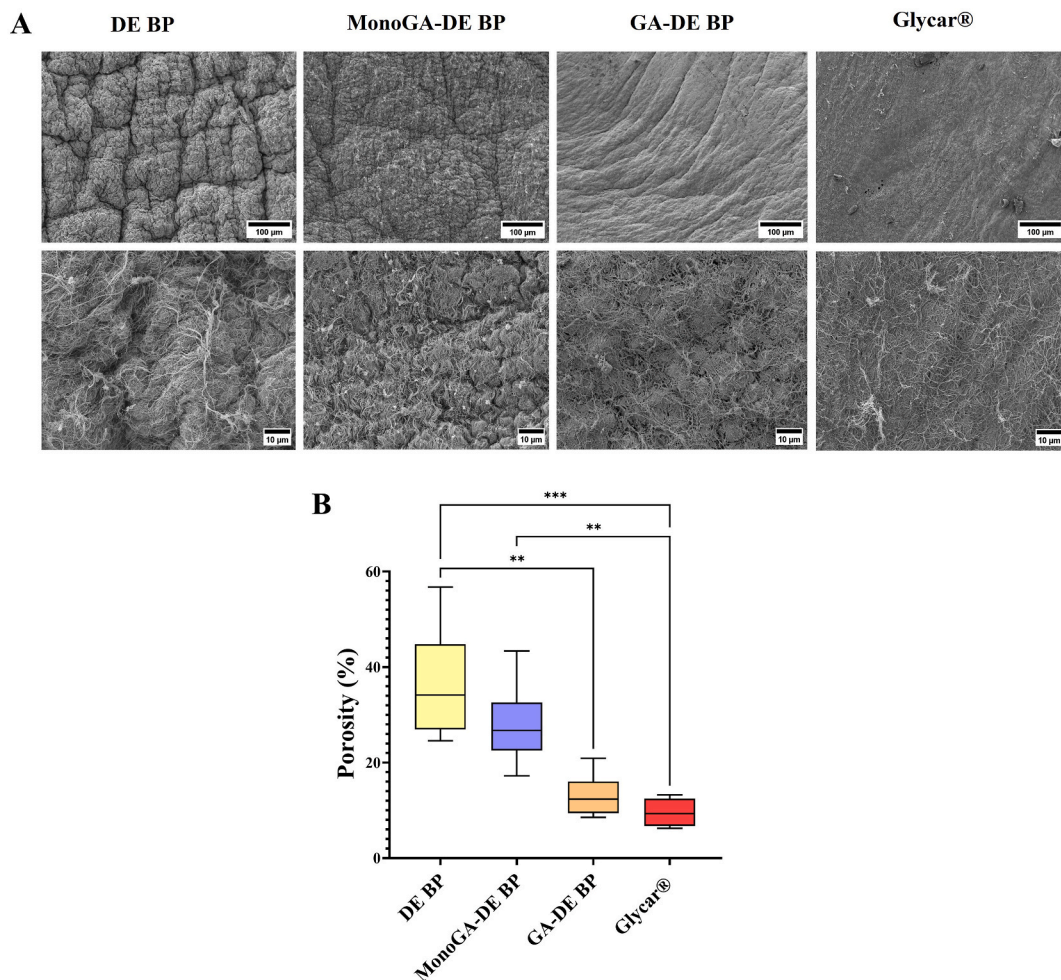


**Fig. 5.** Effect of fixation on the porosity of decellularized bovine pericardium fixed with monomeric GA and GA, compared to a commercial bovine pericardium patch, (A) representative scanning electron microscopy images of different tissue groups (Scales top 100  $\mu$ M, bottom 10  $\mu$ M), (B) Porosity of tissue determined using ImageJ version 1.52t software ( $n = 6$ ). Where: DE BP, decellularized bovine pericardium; MonoGA-DE BP decellularized bovine pericardium fixed with monomeric glutaraldehyde; GA-DE BP decellularized bovine pericardium fixed with glutaraldehyde \*\*\* $p < 0.001$  and \*\* $p < 0.01$ .

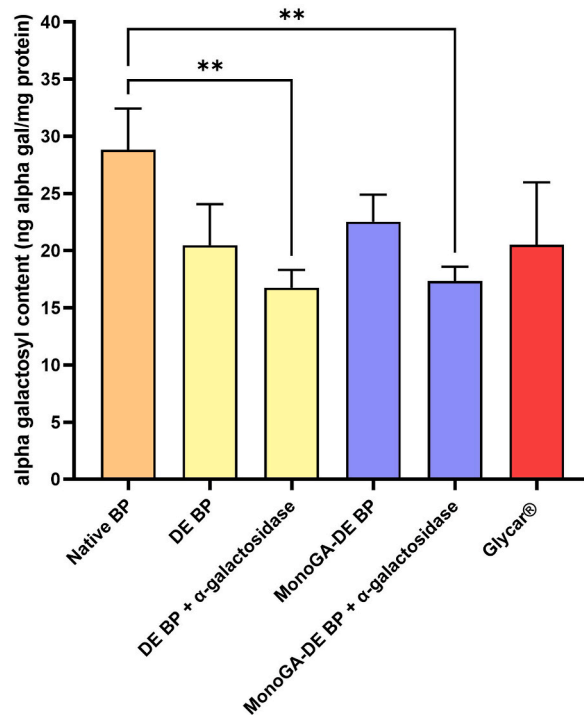


**Fig. 6.** Alpha-galactosyl content of tissue determined through an alpha-galactosyl ELISA (n = 3). Where: Native BP, unprocessed bovine pericardium, DE BP, decellularized bovine pericardium; MonoGA-DE BP, decellularized bovine pericardium fixed with monomeric glutaraldehyde. \*\*p < 0.01.

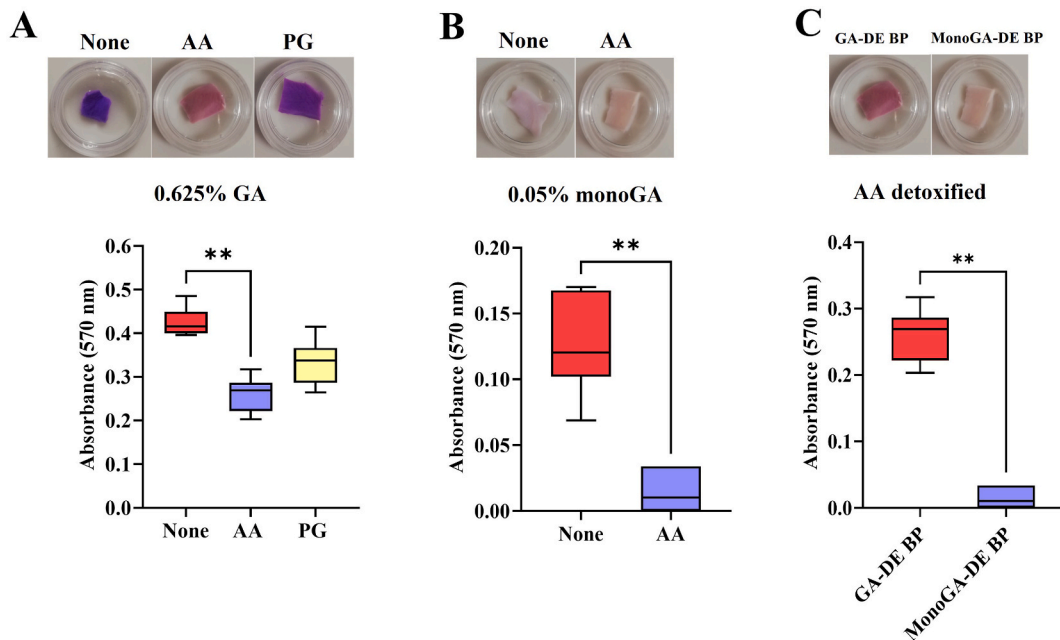


**Fig. 7.** Detoxification efficacy determined with Fuchsin staining, (A-C, top) representative photographs of stained tissue, (A-C bottom) absorbance values for extracted stain (n = 6). None represents non-detoxified 0.625% GA and 0.05% monomeric GA fixed decellularized bovine pericardium, respectively. Where: AA, Amino acid; PG, propylene glycol; GA, glutaraldehyde; monoGA, monomeric glutaraldehyde; GA-DE BP, decellularized bovine pericardium fixed with glutaraldehyde; MonoGA-DE BP, decellularized bovine pericardium fixed with monomeric glutaraldehyde. \*\*p < 0.01.

### 3.6. Detoxification efficacy

Fuchsin staining was used to evaluate the detoxification efficacy. Free aldehyde groups are indicated by a violet color, which occurs when binding occurs between the amino groups of the dye and the free aldehyde groups on the tissue. For 0.625% GA fixed tissue, using propylene glycol or an amino acid solution decreased the intensity of the violet color observed with fuchsin staining (Fig. 7. A top). A significant decrease ( $p = 0.001$ ) in the free aldehyde groups was observed for the amino acid solution (Fig. 7. A bottom). Fixation of tissue with 0.05% monomeric GA produced tissue with a low amount of free aldehydes, as observed by the low intensity of the violet color of the stained tissue. Detoxification with the amino acid solution led to a further decrease in the free aldehyde groups (Fig. 7. B, top); this decrease was found to be significant ( $p = 0.004$ ) (Fig. 7 B, bottom). Monomeric GA fixed tissue detoxified with the amino acid solution (MonoGA-DE BP) had a significantly ( $p = 0.004$ ) lower amount of free aldehyde groups than similarly detoxified GA-fixed tissue (GA-DE BP) (Fig. 7C top and bottom).

### 3.7. Contact and extract toxicity

A decrease in cell growth around the tissue was observed for the GA-DE BP group; cells were also unable to grow at the sides of the tissue, as shown on H&E (Fig. 8. A top). Cell growth was not affected in the MonoGA-DE BP group. Cells were able to grow at the sides of the tissue, as shown on H&E (Fig. 8. A bottom). Extracts from decellularized tissue fixed with 0.625% GA, not detoxified, and not rinsed were highly cytotoxic towards cells (cell viability  $17.88 \pm 6.23\%$ ) (Fig. 8. B). Rinsing the fixed tissue did lead to an increase in the cell viability ( $46.52 \pm 12.39\%$ ), while detoxification led to a further increase in the cell viability ( $60.02 \pm 13.26\%$ ). Extracts from decellularized tissue fixed with 0.05% monomeric GA, not detoxified but rinsed, had a higher percentage of cell viability than GA fixed tissue after detoxification ( $69.77 \pm 25.17\%$ ). Cell viabilities remained significantly lower compared to the controls ( $p < 0.0001$  for positive control, GA-DE BP minus amino acids and GA-DE BP;  $p = 0.0069$  for MonoGA-DE BP minus amino acids) (Fig. 8. B). Extracts from MonoGA-DE BP tissue did not affect cell viability ( $98.76 \pm 14.06\%$ ) compared to control tissue extracts ( $p = 0.9997$ ) (Fig. 8. B).

### 3.8. Host cell infiltration

Collagen from the non-decellularized GA fixed bovine pericardium (Glycar®) was more compact than that of the DE BP group pre-implant (Fig. 9. A). Fixation with 0.05% monomeric GA did lead to the collagen of the decellularized bovine pericardium becoming more condensed compared to the decellularized group. However, it was still wavy with separate interwoven collagen bundles (Fig. 9. A). On H&E, both groups of decellularized tissue (DE BP and MonoGA-DE BP) had higher amounts of host cell infiltration at explant compared to the Glycar® group (Fig. 9. A). The cell counts for the DE BP group were significantly higher ( $p = 0.0029$ ) than that of Glycar® (Fig. 9. B). The cell counts for MonoGA-DE BP were also significantly higher ( $p = 0.0331$ ) than that of Glycar® (Fig. 9. B).

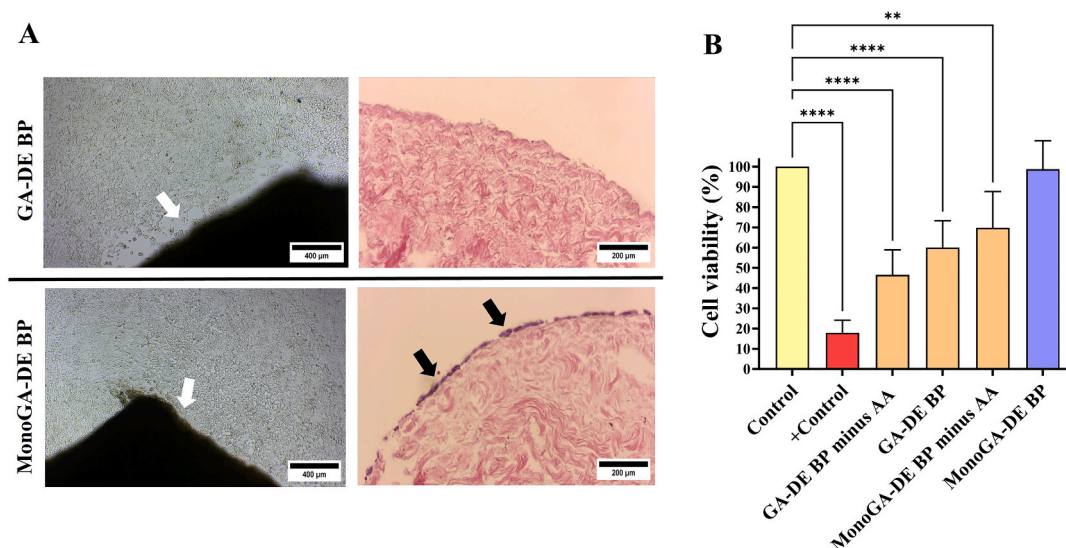


**Fig. 8.** Contact and extract toxicity of fixed and detoxified decellularized bovine pericardium towards HEK-cells, (A) representative light microscope images ( $100 \times$  magnification, scale bars  $400 \mu\text{m}$ ) of contact toxicity assays before tissue removal and following hematoxylin and eosin staining of removed tissue (white arrows show processed tissue, black arrows show cells,  $200 \times$  magnification, scale bars  $200 \mu\text{m}$ ), (B) extract toxicity results determined using the MTT assay ( $n = 6$ ). Results expressed as percentage cell viability relative to native unprocessed tissue (control), positive control represents extracts from decellularized tissue fixed with 0.625% GA, not detoxified and not rinsed. Results expressed as mean  $\pm$  standard deviation ( $n = 6$ ). Where: GA-DE BP, decellularized bovine pericardium fixed with glutaraldehyde; MonoGA-DE BP, decellularized bovine pericardium fixed with monomeric glutaraldehyde; - AA, without amino acid. \*\*\*\* $p < 0.0001$  and \*\* $p < 0.01$ .

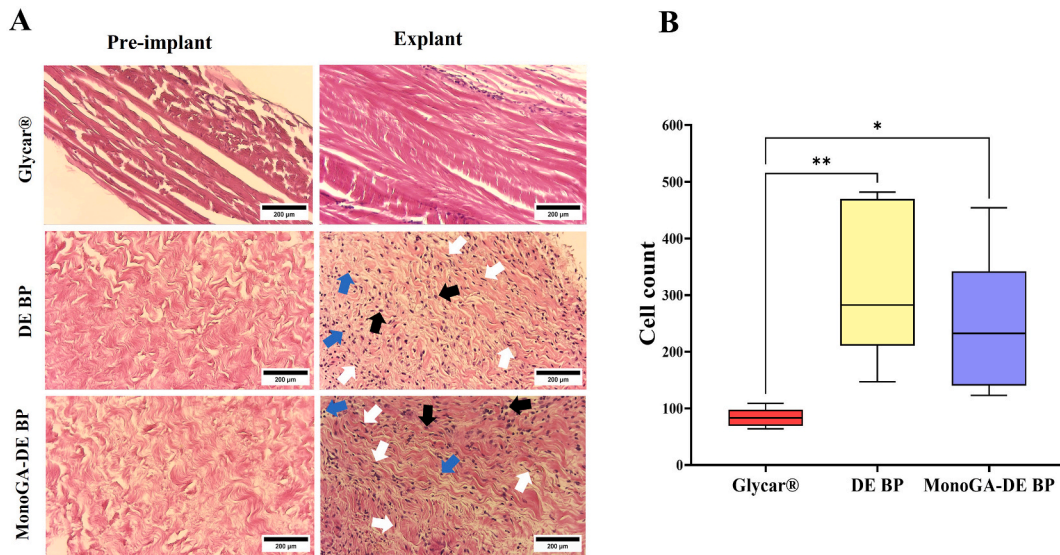


**Fig. 9.** Host cell infiltration following subcutaneous implant of tissue in juvenile male Sprague-Dawley rats (n = 6 per group). (A) Representative hematoxylin and eosin stains (light microscope images) for pre-implanted and explanted tissue (200 × magnification, scale bars 200 μm). Black, blue, and white arrows show infiltrated macrophages, lymphocytes and fibroblasts, respectively. (B) Cell counts done on H&E images using ImageJ version 1.52t software (n = 6). Where: DE BP, decellularized bovine pericardium, MonoGA-DE BP, decellularized bovine pericardium fixed with monomeric glutaraldehyde. \*p < 0.05 and \*\*p < 0.01.

There was no significant difference (p > 0.9999) between the cell counts of the DE BP group (282.5 (range 210.8–470.0)) and the MonoGA-DE BP group (232.5 (range 140.3–342.3)).

### 3.9. Calcification

For all explanted tissue, no calcification was observed on von Kossa (Fig. 10. A). There were no significant differences observed in the quantitative calcium as determined by ICP-MS (p > 0.9999). The medians for the three groups were similar, Glycar® 1.877 μg

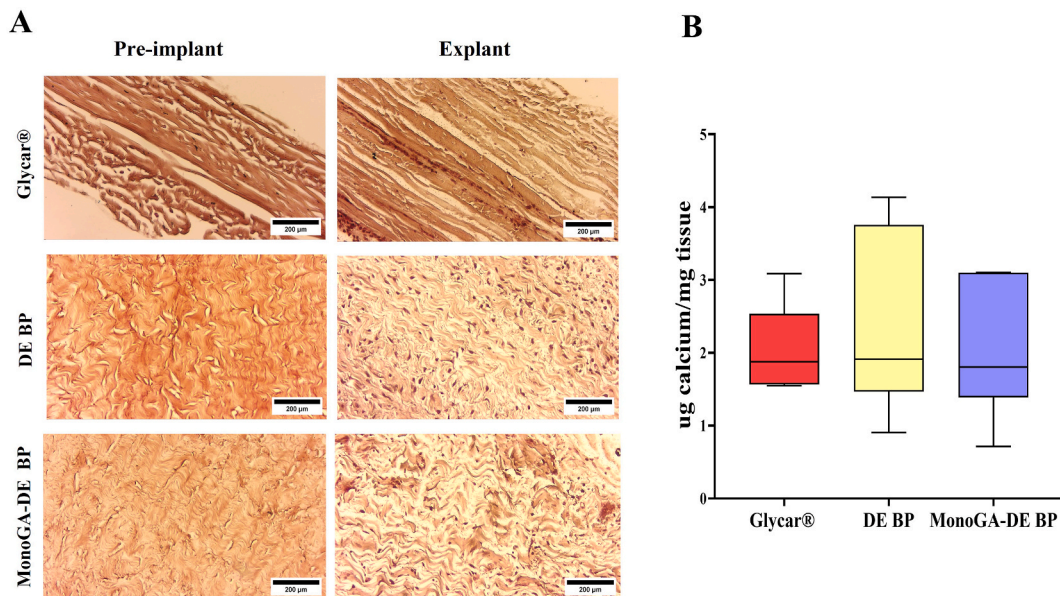


**Fig. 10.** Calcification following subcutaneous implant of tissue in juvenile male Sprague-Dawley rats (n = 6 per group). (A) Representative von Kossa stains (light microscope images) for pre-implanted and explanted tissue (200 × magnification, scale bars 200 μm), (B) Quantitative calcium as determined by ICP-MS (n = 6). Where: DE BP, decellularized bovine pericardium, MonoGA-DE BP, decellularized bovine pericardium fixed with monomeric glutaraldehyde.

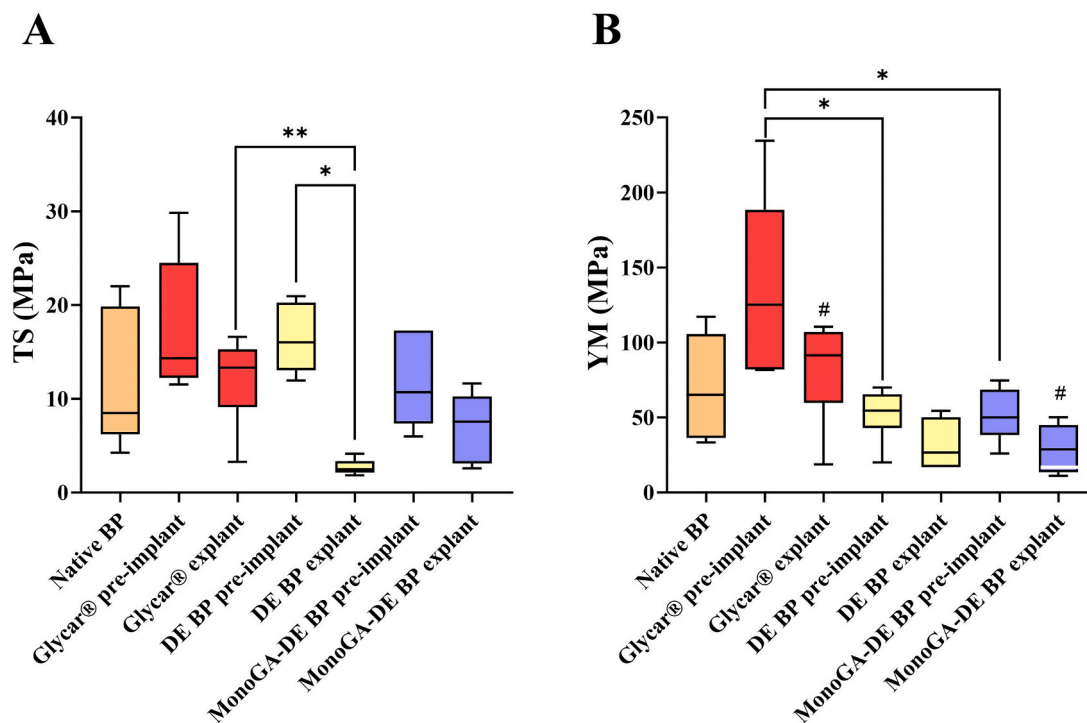


**Fig. 11.** Mechanical properties of tissue at baseline (pre-implant) and at explant following subcutaneous implant in juvenile male Sprague-Dawley rats ( $n = 6$  per group). (A) Tensile strength and (B) Young's modulus. Where: Native BP, unprocessed bovine pericardium; DE BP, decellularized bovine pericardium, MonoGA-DE BP, decellularized bovine pericardium fixed with monomeric glutaraldehyde. \* $p < 0.05$ , \*\* $p < 0.01$  and # $p < 0.05$ .

calcium/mg tissue (range 1.564–2.538), DE BP group 1.921  $\mu\text{g}$  calcium/mg tissue (range 1.464–3.760) and MonoGA-DE BP group 1.804  $\mu\text{g}$  calcium/mg tissue (range 1.386–3.102) (Fig. 10. B).

### 3.10. Mechanical properties

The tensile strength of unprocessed (native) bovine pericardium did not differ significantly from the processed groups at baseline ( $p > 0.05$  in all instances) (Fig. 11. A). The DE BP group had a significantly lower tensile strength at explant ( $p = 0.0313$ ). The DE BP group was also found to have significantly lower tensile strength compared to Glycar® at explant ( $p = 0.0029$ ) (Fig. 11. A). At baseline, the Young's modulus of both decellularized groups (DE BP and MonoGA-DE BP) was significantly lower ( $p = 0.0225$  and  $p = 0.0132$ , respectively) than that of the Glycar® group (Fig. 11. B). At explant, the Young's modulus of the MonoGA-DE BP group was significantly lower ( $p = 0.0386$ ) compared to Glycar® (Fig. 11. B). However, no significant differences were found between the processed tissue and the native unprocessed bovine pericardium.

## 4. Discussion

GA fixation of bovine pericardial tissue remains the industry standard for cardiovascular bioprostheses, despite being linked to cytotoxicity, calcification, and lack of tissue remodeling [10]. Decellularization of xenografts can be considered an alternative means of reducing the antigenicity and immunogenicity of xenographic tissue, such as bovine pericardium, through the removal of donor (foreign) cells and nuclear material. However, decellularization influences the mechanical properties of bovine pericardium, and after implantation, decellularized tissue undergoes rapid resorption due to enzymatic degradation [42,43]. The additional processing of decellularized tissue for use in bioprosthesis with collagen cross-linking agents such as GA might be necessary but comes at the cost of impacting tissue remodeling. In this study, decellularized bovine pericardium was fixed using a low concentration of monomeric GA and detoxified using an amino acid solution. The degree of cross-linking, tissue porosity, enzymatic degradation,  $\alpha$ -gal content, detoxification potential, and cytotoxicity of tissue were evaluated. Processed tissue was subcutaneously implanted in juvenile rats and evaluated on calcification, host cell infiltration, and mechanical properties.

Decellularization was done using a proprietary multi-detergent-based decellularization process [25]. Acellularity was confirmed with H&E. The DNA content was decreased by 90% and was shown to be below 50 ng/mg, which is a criterion of successful decellularization [20]. Following processing, all tissue was culture negative with no growth of fungi, anaerobic and aerobic bacteria. In a previous study by our group, the decellularization technique using the combination of detergents (0.5% SDS, 1% SDC, and 1% TritonX-100) was shown to be synergistic in removing nuclear material. The SDC treatment alone was successful in significantly

reducing the DNA content compared to native bovine pericardium; however, only the combined treatment with all three detergents decreased the DNA content to below 50 ng/mg, with no nuclei or nuclear material visible on 4',6-diamidino-2-phenylindole (DAPI) stain. The combined use of the detergents also did not affect the extracellular matrix (ECM) structure, whereas the use of SDC and SDS separately affected the ECM, with SDS having a more significant impact. TritonX-100 did not cause ECM damage but was ineffective in removing cells and nuclear material. The combined detergent use ultimately resulted in minimal ECM protein and tissue strength loss compared to native pericardium [32]. ECM proteins are conserved among different species and can serve as a scaffold promoting host tissue regeneration through cell attachment, migration, and proliferation [43]. In a subsequent study, the decellularization technique used in this study was also shown to remove lipids [30], which can further contribute to decreasing the calcification potential of the tissue [44]. In another study by our group, the decellularized bovine pericardium, processed using this proprietary method, was implanted into the main pulmonary artery and the descending aorta of juvenile sheep. After six months of implantation, the absence of aneurysm formation was demonstrated with echocardiography despite the tissue not being fixed with GA. Recellularization of the decellularized scaffolds occurred, with no calcification or fibrous encapsulation (pannus) formation [45].

Multi-detergent-based decellularization techniques create cytobiocompatible tissue with tissue-guided regenerative potential [46, 47]. A study by Asgari et al. (2021) investigated the decellularization process for human placenta tissue to create a macroporous scaffold for spermatogonial stem cells homing to be used for reproduction sciences applications. Placenta tissue was decellularized using SDS and TritonX-100 alone and in combination. The combination of 0.5% SDS and 0.5% TritonX-100 for 30 min showed minimal negative effects on ECM components, creating cytobiocompatible, porous tissue that can contribute towards the proliferation, growth, and colony formation of spermatogonial cells [46]. The study by Nikniaz et al. (2021) investigated the combination of SDS and TritonX-100 compared to the combination of SDS, TritonX-100 and ammonium, and the use of SDS alone for the decellularization of ovarian scaffolds for use in regenerative medicine. The survival of preantral follicles from mouse ovaries in an ECM-alginate scaffold was evaluated. The SDS and Triton-X100 group and SDS, TritonX-100 and ammonium group had better cytobiocompatibility, with the porosity structure maintained in all groups [47]. The addition of ammonium might have the added benefit of retaining the glycosaminoglycan content (GAGs) [48], which was found to significantly decreased in bovine pericardium processed using our proprietary multi-detergent based decellularization process [44].

The mechanical strength and transplant efficacy of implanted tissue are compromised by the rapid *in vivo* degradation of decellularized tissue. Also, damage to collagen fibres through enzymatic degradation contributes to BHV degeneration and calcification [49]. Collagen cross-linking methods such as GA fixation can be employed to prevent the degradation of tissue [43]. Commercial GA solutions consist of a mixture of monomers and polymers, and the standard concentration used for fixation is 0.625% [7]. Neethling et al. have shown that ultra-low concentrations of monomeric GA can be used for the adequate cross-linking of decellularized bovine pericardium resulting in enhanced biostability, biocompatibility, and neglectable calcification as evaluated in the implant of tissue in the jugular vein of juvenile sheep [16] and a subcutaneous rat model [50]. Consequently, ADAPT®-treated bovine pericardium (CardioCel®) has been developed. Clinical data in pediatric patients have shown that CardioCel® performs exceptionally well in the short term and is safe and effective for various congenital heart deformations [51]. In the current study, decellularized bovine pericardium was fixed with 0.625% GA or 0.05% monomeric GA plus H<sub>2</sub>O<sub>2</sub>. A decrease in the degree of cross-linking was observed at the lower concentrations of monomeric GA (0.1% and 0.05%) when H<sub>2</sub>O<sub>2</sub> was not included. However, this decrease was not significant ( $p > 0.05$ ). Adding H<sub>2</sub>O<sub>2</sub> to the 0.05% monomeric GA fixation solution, led to a significant increase in the degree of cross-linking achieved with 0.05% monomeric GA, possibly through the synthesis of epoxy aldehydes [52]. The degree of cross-linking achieved with 0.05% monomeric GA plus H<sub>2</sub>O<sub>2</sub> was comparable to when using the highest concentration of GA and monomeric GA (0.625%). The decellularized tissue fixed with the ultra-low concentration (0.05%) of monomeric GA combined with H<sub>2</sub>O<sub>2</sub> was also significantly more resistant to enzymatic degradation than the decellularized unfixed tissue ( $p < 0.05$ ) and comparable to commercial tissue fixed with GA.

Amino acid detoxification was compared to the use of propylene glycol. The amino acid solution was superior in the detoxification of GA-fixed tissue. The amount of free aldehyde groups was inversely proportional to the cytotoxicity of the tissue: the more free aldehydes, the more toxic the tissue, based on both extract and contact toxicity. Similar results were observed by Meuris et al. (2018), who also used an amino acid to neutralize free aldehydes following fixation [34]. The low concentration of monomeric GA combined with H<sub>2</sub>O<sub>2</sub> (without amino acid detoxification) did lead to a decrease in free aldehydes compared to the detoxified GA-fixed tissue. However, the epithelial cells' viability was below 70%, and per the standard ISO 10993-5, a medical device is classified as cytotoxic when the cell viability is reduced to 70%. The fixation with 0.05% monomeric GA plus H<sub>2</sub>O<sub>2</sub> followed by amino acid detoxification did not affect cell viability, as shown with extract toxicity (98.76 ± 14.06%). Furthermore, the processed bovine pericardium did not display contact toxicity, as cells could proliferate and grow in contact with and at the sides of the tissue.

The porosity of a scaffold modulates tissue regeneration by influencing cell functions such as attachment, distribution, migration, and communication [53]. Porous scaffolds with interconnected networks are advantageous in assisting in cell nutrition, proliferation, and migration for tissue vascularization and the formation of new tissue [54]. In the current study, the DE BP group had the highest porosity. The porosity did decrease after fixation, with the only significant differences found on fixation of decellularized tissue with GA (GA-DE BP) and for the Glycar® groups, which was also fixed with GA ( $p < 0.05$ ). Pre-implantation H&E did show that the collagen network for the Glycar® group was compact. The MonoGA-DE BP group had slightly more condensed collagen than the decellularized unfixed group (DE BP); however, the collagen network remained wavy with interwoven, well-separated collagen bundles. Recellularizing tissue scaffolds *in vitro* or through tissue-guided regeneration *in vivo* is vital to creating viable tissue-engineered bioprosthesis. After eight weeks of subcutaneous implantation in juvenile rats, both the decellularized groups (DE BP and MonoGA-DE BP) had significantly higher host cell infiltration than the Glycar® group. The higher degree of host cell infiltration correlates with the higher porosity and the less compact, interwoven, and well-separated collagen bundles observed for the two decellularized groups.

Compared to the DE BP group, the MonoGA-DE BP group had a high crosslinking percentage and was resistant to rapid enzymatic degradation by Type 1A collagenase over a 24-h period. A limitation of *in vitro* enzymatic degradation assays is that they cannot imitate the complex *in vivo* interactions, where numerous cell populations and their secreted enzymes will target the implanted tissue [55–57]. During tissue remodeling, the ECM is subjected to enzymatic degradation by groups of collagenases (a group of enzymes that belong to the family of zinc-dependent proteolytic enzymes, which are known as matrix metalloproteases (MMPs)) [58]. New tissue formation begins 2–10 days after implantation (injury), and tissue remodeling significantly increases 2–3 weeks after implantation [55]. The DE BP group was more susceptible to rapid enzymatic degradation and had a significant decrease in tensile strength after eight weeks of implantation. The MonoGA-DE BP tissue was not susceptible to rapid enzymatic degradation, tensile strength did not decrease after eight weeks of implantation, and cell migration did occur, possibly due to the action MMPs secreted *in vivo*.

Christ et al. (2014) implanted decellularized and decellularized endothelialized porcine aortic wall specimens subcutaneously in rats and found an inflammatory reaction (monocytes and macrophages) and fibroblast infiltration [59]. Inflammatory responses do contribute toward tissue repair and regeneration. Macrophages are characterized as having either an M1 or M2 phenotype. M1 macrophages are linked to a pro-inflammatory response, and M2 macrophages are associated with anti-inflammatory cytokines and ECM production [60]. Brown et al. (2009) evaluated the effect of ECM scaffolds containing cellular components vs. acellular ECM scaffolds upon macrophage phenotype and the relationship between macrophage phenotype and tissue remodeling in Sprague-Dawley rats. Acellular and cellular allogeneic rat ECM scaffolds, and acellular and cellular pig (xenographic) ECM scaffolds were used. It was shown that the acellular scaffolds elicited a predominantly M2-type response resulting in constructive remodeling, while scaffolds containing cellular components (even when autologous) elicited a predominantly M1-type response, resulting in the deposition of dense connective tissue and scarring [61]. In the current study, H&E staining was performed for the general assessment of host cell infiltration. Host cells could penetrate the porous scaffolds, and at explant macrophages, lymphocytes and fibroblasts were present in the tissue of both decellularized groups (DE BP and MonoGA-DE BP). The observation of these cell groups following the subcutaneous implantation of tissue into rodents has also been found for cytobiocompatible porous decellularized placental tissue and decellularized xenogeneic vascular graft materials [46,62]. The presence of macrophages and fibroblasts might allude to a tissue regeneration process. M2 macrophages produce growth factors such as transforming growth factor- $\beta$ 1 (TGF $\beta$ 1) that stimulate the differentiation of fibroblasts into myofibroblasts, and platelet-derived growth factor (PDGF) that stimulates the proliferation of activated ECM-producing myofibroblast [62, 63]. Due to their contractile properties myofibroblasts are characterized by their ability to secrete ECM components and remodel tissue [64]. Further studies should include immunohistochemical analysis to characterize types of cell infiltration and the type of inflammatory response (M2 to M1 ratio).

Xenografts have been introduced as alternatives to human allotransplants and mechanical valves. However, xenoreactive IgG/IgM antibodies, which are directed towards the oligosaccharide residue  $\alpha$ -gal, contribute toward valve degeneration and calcification [65]. GA fixation has been shown to reduce but not completely mask the  $\alpha$ -gal epitope with the detection of the  $\alpha$ -gal epitope in GA-fixed heart valve prosthesis used clinically [66]. A decellularization process that includes the use of Triton-X 100, SDC, and the detergent IGEPAL CA-360 has been shown to completely remove the  $\alpha$ -gal epitope from porcine tissue, as detected through the use of laser scanning microscopy with high-affinity isolectin [22]. However, when another research group employed the same decellularization method and a specific  $\alpha$ -gal antibody ELISA assay was performed, it was shown that the amount of  $\alpha$ -gal in the porcine tissue was only halved [67]. In the current study, using a quantitative ELISA method, a decrease in the  $\alpha$ -gal content was observed in both the unfixed and monomeric GA fixed decellularized bovine pericardium, and the commercial GA fixed tissue (Glycar®) compared to the fresh unprocessed native bovine pericardium. This decrease was, however, not found to be significant ( $p > 0.05$ ). Results indicated that the fixation of decellularized bovine pericardium with monomeric GA did not further decrease the  $\alpha$ -Gal content. The additional  $\alpha$ -galactosidase enzyme treatment significantly decreased the  $\alpha$ -gal content for unfixed and monomeric GA fixed decellularized tissue ( $p < 0.05$ ). However, a low concentration (0.5 U/mg) of the  $\alpha$ -galactosidase enzyme was used. The process should be further optimized and included in the processing process to adequately reduce the  $\alpha$ -Gal content and diminish the immune response when used clinically.

GA fixation of bioprosthesis prevents repopulation of the ECM with host cells and leads to structural deterioration, calcification, and inevitable valve failure [3,10]. In this study, Glycar® tissue, fixed with GA, displayed limited host cell infiltration. However, at explant, none of the implanted tissue groups showed calcification on von Kossa staining. Low calcium levels were found with quantitative calcium analysis, with no significant differences in the calcification of the differently processed tissues. Removal of cellular components from xenografts might limit the immunological response from the recipient, but mechanical properties such as strength and stiffness (Young's modulus) have to be maintained [68]; therefore, additional fixation and stabilization of the collagen scaffold following decellularization might be required. Also, an increase in porosity leads to a decrease in stiffness and strength which can cause the tissue scaffold to become vulnerable to breakage [54]. This study demonstrated no significant differences between the tensile strengths of the processed tissue (DE BP, MonoGA-DE BP and Glycar® groups) and native unprocessed bovine pericardium at pre-implant. At explant, the strength of the DE BP group decreased significantly ( $p < 0.05$ ). When comparing the stiffness of the processed tissue groups to that of native unprocessed bovine pericardium, no significant differences were found. There was no significant difference in the stiffness of each tissue group at pre-implant and explant.

## 5. Limitations of the study

The subcutaneous rat model used in this study provides permanent contact of implanted tissue to host tissue to ease host cell infiltration. This model does provide information on the biocompatibility of processed tissue for use in cardiovascular bioprostheses; however, the model suffers from the absence of mechanical stress. Therefore, the functionality of the tissue should be further investigated in the juvenile sheep model, which allows the test to be performed in the systemic circulation.

## 6. Conclusion

The main findings of the study are summarized in the graphical abstract (available online). GA is routinely used for the fixation of bovine pericardium at a standard concentration of 0.625%. Propylene glycol is an industry standard for neutralizing unbound aldehyde groups that might lead to calcification and cytotoxicity, ultimately preventing tissue degradation. The current study showed that bovine pericardium, which was decellularized using a multi-detergent method, fixed with a low concentration (0.05%) of monomeric GA in combination with H<sub>2</sub>O<sub>2</sub> and detoxified with an amino acid solution, retained its mechanical properties and was resistant to rapid enzymatic degradation. The processed tissue also has the potential for tissue regeneration due to a higher level of porosity, no cytotoxicity, and better host cell infiltration compared to GA fixed tissue. Furthermore, the fixation and detoxification process was successful in preventing calcification. The developed technique can be considered for processing decellularized bovine pericardium with tissue-guided regenerative potential for use in cardiovascular bioprostheses. Although the antigenicity did decrease, the use of the  $\alpha$ -galactosidase enzyme in the fixation and detoxification process should be investigated to reduce the  $\alpha$ -gal epitope further, diminish the immune response and ensure biocompatibility for clinical use.

## Author contribution statement

Angélique Lewies: Conceived and designed the experiments; Performed the experiments; Analyzed and interpreted the data; Wrote the paper.

Lezelle Botes: Analyzed and interpreted the data; Wrote the paper.

Johannes Jacobus van den Heever: Performed experiments; Analyzed and interpreted the data.

Pascal Maria Dohmen: Conceived and designed the experiments.

Francis Edwin Smit: Conceived and designed the experiments; Contributed reagents, materials, analysis tools or data; Wrote the paper.

## Funding statement

Angélique Lewies received funding from the Open Access Publication Fund (OAPF), University of the Free State.

## Data availability statement

Data will be made available on request.

## Declaration of competing interest

The authors declare that they have no known competing financial interests or personal relationships that could have appeared to influence the work reported in this paper.

## Acknowledgments

The authors would like to thank the Department of Anatomical Pathology, UFS, for assistance with histology analyses; the Centre for Confocal and Electron Microscopy, UFS, for assistance with SEM analyses, and the Animal Research Centre, UFS, for assistance with *in vivo* experiments. The graphical abstract was created with [Biorender.com](https://www.biorender.com)

## References

- [1] P. Singhal, A. Luk, J. Butany, Bioprosthetic Heart Valves: Impact of Implantation on Biomaterials, 2013, ISRN Biomaterials, 2013, 728791, <https://doi.org/10.5402/2013/728791>.
- [2] K.Y.C. Li, Bioprosthetic heart valves: upgrading a 50-year old technology, *Frontiers in Cardiovascular Medicine* 6 (2019).
- [3] R.A. Manji, W. Lee, D.K.C. Cooper, Xenograft bioprosthetic heart valves: past, present and future, *Int. J. Surg.* 23 (Pt B) (2015) 280–284, <https://doi.org/10.1016/j.ijvs.2015.07.009>.
- [4] S.J. Head, M. Çelik, A.P. Kappetein, Mechanical versus bioprosthetic aortic valve replacement, *Eur. Heart J.* 38 (28) (2017) 2183–2191, <https://doi.org/10.1093/eurheartj/ehx141>.
- [5] P. Sinha, D. Zurakowski, T.K. Kumar, D. He, C. Rossi, R.A. Jonas, Effects of glutaraldehyde concentration, pretreatment time, and type of tissue (porcine versus bovine) on post-implantation calcification, *J. Thorac. Cardiovasc. Surg.* 143 (1) (2012) 224–227, <https://doi.org/10.1016/j.jtcvs.2011.09.043>.
- [6] C. Hilger, J. Fischer, F. Wölbing, T. Biedermann, Role and mechanism of Galactose- $\alpha$ -1,3-Galactose in the elicitation of delayed anaphylactic reactions to red meat, *Curr. Allergy Asthma Rep.* 19 (1) (2019) 3, <https://doi.org/10.1007/s11882-019-0835-9>.
- [7] D.M. Sánchez, D.M. Gaitán, A.F. León, J. Mugnier, J.C. Briceño, Fixation of vascular grafts with increased glutaraldehyde concentration enhances mechanical properties without increasing calcification, *Am. Soc. Artif. Intern. Organs J.* 53 (3) (2007) 257–262, <https://doi.org/10.1097/MAT.0b013e318033a68>.
- [8] H.C. Ott, T.K. Rajab, Chapter 13 - tissue-derived matrices, in: S.J. Lee, J.J. Yoo, A. Atala (Eds.), *In Situ Tissue Regeneration*, Academic Press, Boston, 2016, pp. 229–250.
- [9] A. López Marco, O. Nawaytou, U.O. Von Oppell, Late aortic aneurysm after supravalvar aortic stenosis repaired with autologous pericardial patch, *Ann. Thorac. Surg.* 95 (1) (2013) 346–348.
- [10] P.R. Umashankar, P.V. Mohanan, T.V. Kumari, Glutaraldehyde treatment elicits toxic response compared to decellularization in bovine pericardium, *Toxicol. Int.* 19 (1) (2012) 51–58, <https://doi.org/10.4103/0971-6580.94513>.
- [11] A. Oryan, A. Kamali, A. Moshiri, H. Baharvand, H. Daemi, Chemical cross-linking of biopolymeric scaffolds: current knowledge and future directions of cross-linked engineered bone scaffolds, *Int. J. Biol. Macromol.* 107 (Pt A) (2018) 678–688, <https://doi.org/10.1016/j.ijbiomac.2017.08.184>.

- [12] K.M. Kim, G.A. Herrera, H.D. Battarbee, Role of glutaraldehyde in calcification of porcine aortic valve fibroblasts, *Am. J. Pathol.* 154 (3) (1999) 843–852, [https://doi.org/10.1016/S0002-9440\(10\)65331-X](https://doi.org/10.1016/S0002-9440(10)65331-X).
- [13] R.F. Siddiqui, J.R. Abraham, J. Butany, Bioprosthetic heart valves: modes of failure, *Histopathology* 55 (2) (2009) 135–144, <https://doi.org/10.1111/j.1365-2559.2008.03190.x>.
- [14] Z. Jiang, Z. Wu, D. Deng, J. Li, X. Qi, M. Song, et al., Improved cytocompatibility and reduced calcification of glutaraldehyde-crosslinked bovine pericardium by modification with Glutathione, *Front. Bioeng. Biotechnol.* 10 (2022), 844010, <https://doi.org/10.3389/fbioe.2022.844010>.
- [15] E. Seifter, R.W.M. Frater, *Anticalcification Treatment for Aldehyde-Tanned Biological Tissue*, Albert Einstein College of Medicine of Yeshiva University (Bronx, NY), United States, 1995.
- [16] W.M. Neethling, S. Yadav, A.J. Hodge, R. Glancy, Enhanced biostability and biocompatibility of decellularized bovine pericardium, cross-linked with an ultra-low concentration monomeric aldehyde and treated with ADAPT, *J. Heart Valve Dis.* 17 (4) (2008) 456–463, discussion 64.
- [17] N. Vyavahare, D. Hirsch, E. Lerner, J.Z. Baskin, F.J. Schoen, R. Bianco, et al., Prevention of bioprosthetic heart valve calcification by ethanol preincubation. Efficacy and mechanisms, *Circulation* 95 (2) (1997) 479–488, <https://doi.org/10.1161/01.cir.95.2.479>.
- [18] C. Collatusso, J.G. Roderjan, L. de Noronha, A. Klosowski, P.H. Suss, L.C. Guarita-Souza, et al., Decellularization as a method to reduce calcification in bovine pericardium bioprosthetic valves, *Interact. Cardiovasc. Thorac. Surg.* (2019), <https://doi.org/10.1093/icvts/ivz041>.
- [19] C. Collatusso, J.G. Roderjan, E.D. Vieira, N.I. Myague, L. Noronha, F.D. Costa, Decellularization as an anticalcification method in stentless bovine pericardium valve prosthesis: a study in sheep, *Rev. Bras. Cir. Cardiovasc.* 26 (3) (2011) 419–426, <https://doi.org/10.5935/1678-9741.20110017>.
- [20] P.M. Crapo, T.W. Gilbert, S.F. Badylak, An overview of tissue and whole organ decellularization processes, *Biomaterials* 32 (12) (2011) 3233–3243, <https://doi.org/10.1016/j.biomaterials.2011.01.057>.
- [21] N. Li, Y. Li, D. Gong, C. Xia, X. Liu, Z. Xu, Efficient decellularization for bovine pericardium with extracellular matrix preservation and good biocompatibility, *Interact. Cardiovasc. Thorac. Surg.* 26 (5) (2018) 768–776, <https://doi.org/10.1093/icvts/ivx416>.
- [22] M.T. Kasimir, E. Rieder, G. Seebacher, E. Wolner, G. Weigel, P. Simon, Presence and elimination of the xenoantigen gal (alpha1, 3) gal in tissue-engineered heart valves, *Tissue Eng.* 11 (7–8) (2005) 1274–1280, <https://doi.org/10.1089/ten.2005.11.1274>.
- [23] L. Iop, G. Gerosa, Guided tissue regeneration in heart valve replacement: from preclinical research to first-in-human trials, *BioMed Res. Int.* 2015 (2015), 432901, <https://doi.org/10.1155/2015/432901>.
- [24] I.K. Ko, S.J. Lee, A. Atala, J.J. Yoo, In situ tissue regeneration through host stem cell recruitment, *Exp. Mol. Med.* 45 (2013) e57, <https://doi.org/10.1038/emm.2013.118>.
- [25] D. Bester, F.E. Smit, J.J. Van Den Heever, L. Botes, P.M.C.E. Dohmen, *Detoxification and Stabilization of Implantable or Transplantable Biological Material*. Patent: 16702008 vols. 0–1455, EU, 2017.
- [26] A. Abay, G. Simionato, R. Chachanidze, A. Bogdanova, L. Hertz, P. Bianchi, L. Kaestner, Glutaraldehyde - a subtle tool in the investigation of healthy and pathologic red blood cells, *Front. Physiol.* 10 (2019) 514, <https://doi.org/10.3389/fphys.2019.00514>.
- [27] S. Kirkeby, P. Jakobsen, D. Moe, Glutaraldehyde - "pure and impure." A spectroscopic investigation of two commercial glutaraldehyde solutions and their reaction products with amino acids, *Anal. Lett.* 20 (2) (1987) 303–315, <https://doi.org/10.1080/00032718708064567>.
- [28] J.J. van den Heever, C.J. Jordaan, A. Lewies, J. Goedhals, D. Bester, L. Botes, et al., Impact of three different processing techniques on the strength and structure of juvenile ovine pulmonary homografts, *Polymers* 14 (15) (2022), <https://doi.org/10.3390/polym14153036>.
- [29] H.Y. Cheung, M.R. Brown, Evaluation of glycine as an inactivator of glutaraldehyde, *J. Pharm. Pharmacol.* 34 (4) (1982) 211–214, <https://doi.org/10.1111/j.2042-7158.1982.tb04230.x>.
- [30] L. Cui, J. Jia, Y. Guo, Y. Liu, P. Zhu, Preparation and characterization of IPN hydrogels composed of chitosan and gelatin cross-linked by genipin, *Carbohydr. Polym.* 99 (2014) 31–38, <https://doi.org/10.1016/j.carbpol.2013.08.048>.
- [31] S. Moore, W.H. Stein, A modified ninhydrin reagent for the photometric determination of amino acids and related compounds, *J. Biol. Chem.* 211 (2) (1954) 907–913.
- [32] L. Laker, P.M. Dohmen, F.E. Smit, Synergy in a detergent combination results in superior decellularized bovine pericardial extracellular matrix scaffolds, *J. Biomed. Mater. Res. B Appl. Biomater.* (2020), <https://doi.org/10.1002/jbm.b.34588>.
- [33] Y. Lu, A. Shao, Y. Shan, H. Zhao, M. Leiguo, Y. Zhang, et al., A standardized quantitative method for detecting remnant alpha-Gal antigen in animal tissues or animal tissue-derived biomaterials and its application, *Sci. Rep.* 8 (1) (2018), 15424, <https://doi.org/10.1038/s41598-018-32959-1>.
- [34] B. Meuris, H. De Praetere, M. Strasly, P. Trabucco, J.C. Lai, P. Verbrugge, et al., A novel tissue treatment to reduce mineralization of bovine pericardial heart valves, *J. Thorac. Cardiovasc. Surg.* 156 (1) (2018) 197–206, <https://doi.org/10.1016/j.jtcvs.2018.01.099>.
- [35] A. Lewies, J.F. Wentzel, H.C. Miller, L.H. Du Plessis, The antimicrobial peptide nisin Z induces selective toxicity and apoptotic cell death in cultured melanoma cells, *Biochimie* 144 (2018) 28–40, <https://doi.org/10.1016/j.biochi.2017.10.009>.
- [36] N. Percie du Sert, V. Hurst, A. Ahluwalia, S. Alam, M.T. Avey, M. Baker, et al., The ARRIVE guidelines 2.0: updated guidelines for reporting animal research, *PLoS Biol.* 18 (7) (2020), e3000410, <https://doi.org/10.1371/journal.pbio.3000410>.
- [37] J.C. Seely, A brief review of kidney development, maturation, developmental abnormalities, and drug toxicity: juvenile animal relevancy, *J. Toxicol. Pathol.* 30 (2) (2017) 125–133, <https://doi.org/10.1293/tox.2017-0006>.
- [38] J.D. Bancroft, A. Stevens, *Theory and Practice of Histological Techniques*, third ed., Churchill Livingstone, Edinburgh, 1990.
- [39] J.D. Bancroft, A. Stevens, *Theory and Practice of Histological Techniques*, third ed., Churchill Livingstone, Edinburgh, 1991.
- [40] J.J. van den Heever, C.J. Jordaan, A. Lewies, D. Bester, J. Goedhals, L. Botes, et al., Comparison of the function and structural integrity of cryopreserved pulmonary homografts versus decellularized pulmonary homografts after 180 days implantation in the juvenile ovine model, *Cell Tissue Bank.* 23 (2) (2022) 347–366, <https://doi.org/10.1007/s10561-021-09948-2>.
- [41] W.N. Arifin, W.M. Zahiruddin, Sample size calculation in animal studies using resource equation approach, *Malays. J. Med. Sci.* 24 (5) (2017) 101–105, <https://doi.org/10.21315/mjms2017.24.5.11>.
- [42] E. Rémi, N. Khelil, I. Di Centa, C. Roques, M. Ba, F. Medjahed-Hamidi, et al., Pericardial processing: challenges, outcomes and future prospects, in: R. Pignatello (Ed.), *Biomaterials Science and Engineering*, IntechOpen, 2011.
- [43] Q. Yao, Y.W. Zheng, H.L. Lin, Q.H. Lan, Z.W. Huang, L.F. Wang, et al., Exploiting cross-linked decellularized matrix to achieve uterus regeneration and construction, *Artif. Cells, Nanomed. Biotechnol.* 48 (1) (2020) 218–229, <https://doi.org/10.1080/21691401.2019.1699828>.
- [44] L. Laker, P.M. Dohmen, F.E. Smit, The sequential effects of a multifactorial detergent based decellularization process on bovine pericardium, *Biomed Phys Eng Express* 6 (6) (2020), <https://doi.org/10.1088/2057-1976/abb5e9>.
- [45] L. Botes, L. Laker, P.M. Dohmen, J.J. van den Heever, C.J. Jordaan, A. Lewies, et al., Advantages of decellularized bovine pericardial scaffolds compared to glutaraldehyde fixed bovine pericardial patches demonstrated in a 180-day implant ovine study, *Cell Tissue Bank.* (2022), <https://doi.org/10.1007/s10561-021-09988-8>.
- [46] F. Asgari, H.R. Asgari, M. Najafi, B.S. Eftekhari, M. Vardiani, M. Gholipourmalekabadi, et al., Optimization of decellularized human placental macroporous scaffolds for spermatogonial stem cells homing, *J. Mater. Sci. Mater. Med.* 32 (5) (2021) 47, <https://doi.org/10.1007/s10856-021-06517-7>.
- [47] H. Nikniaz, Z. Zandieh, M. Nouri, N. Daei-Farshbaf, R. Aflatoonian, M. Gholipourmalekabadi, et al., Comparing various protocols of human and bovine ovarian tissue decellularization to prepare extracellular matrix-alginate scaffold for better follicle development in vitro, *BMC Biotechnol.* 21 (1) (2021) 8, <https://doi.org/10.1186/s12896-020-00658-3>.
- [48] R.E. Coronado, M. Somaraki-Cormier, S. Natesan, R.J. Christy, J.L. Ong, G.A. Halff, Decellularization and solubilization of porcine liver for use as a substrate for porcine hepatocyte culture: method optimization and comparison, *Cell Transplant.* 26 (12) (2017) 1840–1854, <https://doi.org/10.1177/0963689717742157>.
- [49] A.E. Kostyunin, A.E. Yuzhalin, M.A. Rezvova, E.A. Ovcharenko, T.V. Glushkova, A.G. Kutikhin, Degeneration of bioprosthetic heart valves: update 2020, *J. Am. Heart Assoc.* 9 (19) (2020), e018506, <https://doi.org/10.1161/JAHA.120.018506>.

- [50] W. Neethling, C. Brizard, L. Firth, R. Glancy, Biostability, durability and calcification of cryopreserved human pericardium after rapid glutaraldehyde-stabilization versus multistep ADAPT(R) treatment in a subcutaneous rat model, *Eur. J. Cardio. Thorac. Surg.* 45 (4) (2014) e110–e117, <https://doi.org/10.1093/ejcts/ezt623>.
- [51] G. Strange, C. Brizard, T.R. Karl, L. Neethling, An evaluation of Admedus' tissue engineering process-treated (ADAPT) bovine pericardium patch (CardioCel) for the repair of cardiac and vascular defects, *Expet Rev. Med. Dev.* 12 (2) (2015) 135–141, <https://doi.org/10.1586/17434440.2015.985651>.
- [52] C. Peracchia, B.S. Mittler, Fixation by means of glutaraldehyde-hydrogen peroxide reaction products, *J. Cell Biol.* 53 (1) (1972) 234–238, <https://doi.org/10.1083/jcb.53.1.234>.
- [53] Q.L. Loh, C. Choong, Three-dimensional scaffolds for tissue engineering applications: role of porosity and pore size, *Tissue Eng., Part B* 19 (6) (2013) 485–502, <https://doi.org/10.1089/ten.TEB.2012.0437>.
- [54] P. Yadav, G. Beniwal, K.K. Saxena, A review on pore and porosity in tissue engineering, *Mater. Today: Proc.* 44 (2021) 2623–2628, <https://doi.org/10.1016/j.matpr.2020.12.661>.
- [55] L.M. Delgado, Y. Bayon, A. Pandit, D.I. Zeugolis, To cross-link or not to cross-link? Cross-linking associated foreign body response of collagen-based devices, *Tissue Eng., Part B* 21 (3) (2015) 298–313, <https://doi.org/10.1089/ten.TEB.2014.0290>.
- [56] D. Das, Z. Zhang, T. Winkler, M. Mour, C. Gunter, M. Morlock, A.F. Schilling, Bioresorption and degradation of biomaterials, *Adv. Biochem. Eng. Biotechnol.* 126 (2012) 317–333, [https://doi.org/10.1007/10\\_2011\\_119](https://doi.org/10.1007/10_2011_119).
- [57] G.J. Laurent, Dynamic state of collagen: pathways of collagen degradation in vivo and their possible role in regulation of collagen mass, *Am. J. Physiol.* 252 (1 Pt 1) (1987) C1–C9, <https://doi.org/10.1152/ajpcell.1987.252.1.C1>.
- [58] D. Singh, S.K. Srivastava, T.K. Chaudhuri, G. Upadhyay, Multifaceted role of matrix metalloproteinases (MMPs), *Front. Mol. Biosci.* 2 (2015) 19, <https://doi.org/10.3389/fmolb.2015.00019>.
- [59] T. Christ, P.M. Dohmen, S. Holinski, M. Schönau, G. Heinze, W. Konertz, Suitability of the rat subdermal model for tissue engineering of heart valves, *Med Sci Monit Basic Res* 20 (2014) 194–199, <https://doi.org/10.12659/MSMBR.893088>.
- [60] M.M. Alvarez, J.C. Liu, G. Trujillo-de Santiago, B.H. Cha, A. Vishwakarma, A.M. Ghaemmaghami, et al., Delivery strategies to control inflammatory response: modulating M1-M2 polarization in tissue engineering applications, *J. Contr. Release* 240 (2016) 349–363, <https://doi.org/10.1016/j.jconrel.2016.01.026>.
- [61] B.N. Brown, J.E. Valentin, A.M. Stewart-Akers, G.P. McCabe, S.F. Badyak, Macrophage phenotype and remodeling outcomes in response to biologic scaffolds with and without a cellular component, *Biomaterials* 30 (8) (2009) 1482–1491, <https://doi.org/10.1016/j.biomaterials.2008.11.040>.
- [62] I. Stöwe, J. Pissarek, P. Moosmann, A. Pröhl, S. Pantermehl, J. Bielenstein, et al., Ex vivo and in vivo analysis of a novel porcine aortic patch for vascular reconstruction, *Int. J. Mol. Sci.* 22 (14) (2021), <https://doi.org/10.3390/ijms22147623>.
- [63] P.J. Murray, T.A. Wynn, Protective and pathogenic functions of macrophage subsets, *Nat. Rev. Immunol.* 11 (11) (2011) 723–737, <https://doi.org/10.1038/nri3073>.
- [64] J. Davis, J.D. Molkenin, Myofibroblasts: trust your heart and let fate decide, *J. Mol. Cell. Cardiol.* 70 (2014) 9–18, <https://doi.org/10.1016/j.yjmcc.2013.10.019>.
- [65] K.Z. Konakci, B. Bohle, R. Blumer, W. Hoetzenecker, G. Roth, B. Moser, et al., Alpha-Gal on bioprostheses: xenograft immune response in cardiac surgery, *Eur. J. Clin. Invest.* 35 (1) (2005) 17–23, <https://doi.org/10.1111/j.1365-2362.2005.01441.x>.
- [66] F. Naso, A. Gandaglia, T. Bottio, V. Tarzia, M.B. Nottle, A.J. d'Apice, et al., First quantification of alpha-Gal epitope in current glutaraldehyde-fixed heart valve bioprostheses, *Xenotransplantation* 20 (4) (2013) 252–261, <https://doi.org/10.1111/xen.12044>.
- [67] M. Spina, F. Naso, I. Zancan, L. Iop, M. Dettin, G. Gerosa, Biocompatibility issues of next Generation decellularized bioprosthetic devices, *Conference Papers in Science* 2014 (2014), 869240, <https://doi.org/10.1155/2014/869240>.
- [68] W. Erdbrugger, W. Konertz, P.M. Dohmen, S. Posner, H. Ellerbrok, O.E. Brodde, et al., Decellularized xenogenic heart valves reveal remodeling and growth potential in vivo, *Tissue Eng.* 12 (8) (2006) 2059–2068, <https://doi.org/10.1089/ten.2006.12.2059>.